Journal of Cellular Biochemistry 45:101–111 (1991)

Parathyroid Hormone Promotes the Disassembly of Cytoskeletal Actin and Myosin in Cultured Osteoblastic Cells: Mediation by Cyclic AMP

John J. Egan, Gloria Gronowicz, and Gideon A. Rodan

Laboratory of Cellular and Developmental Biology, National Institutes of Diabetes, Digestive, and Kidney Diseases, National Institutes of Health, Bethesda, Maryland 20891 (J.J.E.); Department of Orthopedic Surgery, The University of Connecticut Health Center, School of Medicine, Farmington, Connecticut 06032 (G.G.); Merck, Sharp and Dohme Research Laboratories, West Point, Pennsylvania 19486 (G.A.R.)

Abstract Parathyroid hormone (PTH) alters the shape of osteoblastic cells both in vivo and in vitro. In this study, we examined the effect of PTH on cytoskeletal actin and myosin, estimated by polyacrylamide gel electrophoresis of Triton X-100 (1%) nonextractable proteins. After 2–5 minutes, PTH caused a rapid and transient decrease of 50–60% in polymerized actin and myosin associated with the Triton X-100 nonextractable cytoskeleton. Polymerized actin returned to control levels by 30 min. The PTH effect was dose-dependent with an IC_{50} of about 1 nM, and was partially inhibited by the (3–34) PTH antagonist. PTH caused a rapid transient rise in cyclic AMP (cAMP) in these cells that peaked at 4 min, while the nadir in cytoskeletal actin and myosin was recorded around 5 min. The intracellular calcium chelator Quin-2/AM (10 μM) also decreased cytoskeletal actin and myosin, to the same extent as did PTH (100 nM). To distinguish between cAMP elevation and Ca^{++} reduction as mediators of PTH action, we measured the phosphorylation of the 20 kD (PI 4.9) myosin light chain in cells preincubated with [^{32}P]-orthophosphate. The phosphorylation of this protein decreased within 2–3 min after PTH addition and returned to control levels after 5 min. The calcium ionophore A-23187 did not antagonize this PTH effect. Visualization of microfilaments with rhodamine-conjugated phalloidin showed that PTH altered the cytoskeleton by decreasing the number of stress fibers. These changes in the cytoskeleton paralleled changes in the shape of the cells from a spread configuration to a stellate form with retracting processes. The above findings indicate that the alteration in osteoblast shape produced by PTH involve relatively rapid and transient changes in cytoskeletal organization that appear to be mediated by cAMP.

Key words: parathyroid hormone, cyclic AMP, osteoblasts, actin, myosin, calcium

Many hormones including TSH [1,2], FSH [3], ACTH [4], and parathyroid hormone (PTH) [5–7] alter the shape of their target cells as part of their "pleiotropic" effects. These hormones stimulate adenylate cyclase. Similarly, cyclic AMP (cAMP) and its analog dibutyryl cAMP were shown to cause shape changes in various cells [8–10]. Usually, cells change from a spread-out to a stellate morphology, which is often described as cytoplasmic retraction. This change is thought to involve cytoskeletal changes, primarily in microfilaments [11].

The role of cAMP in the regulation of the cytoskeleton has been extensively studied in smooth muscle and platelets [12]. For actin and myosin to interact in nonmuscle vertebrate cells, the 20 kD myosin light chain, MLC_{20}, must be phosphorylated [13,14]. Phosphorylation of MLC_{20} is catalyzed by myosin light chain kinase (MLCK), a calcium and calmodulin activated enzyme [15]. This process is attenuated by a cAMP-dependent protein kinase, which phosphorylates the MLCK, reduces its affinity for calcium-calmodulin, and decreases its enzymatic activity [16]. An alternate mechanism whereby cAMP may attenuate this process involves the extrusion of cytosolic calcium. In platelets, PGD_2 and forskolin, which increase cAMP, reduced both cytosolic calcium and MLC_{20} phosphorylation, while causing actomyosin disassembly [17].

In a related report [18], we found an inverse relationship between actin and myosin associated with the cytoskeleton (Triton X-100 nonextractable) and the cellular cAMP level, which rose with increasing cell density in culture. In

Received June 7, 1990; accepted October 3, 1990.

this study, we examined the effect of PTH, which modulates cAMP levels and calcium fluxes in osteoblastic cells, on polymerized cytoskeletal proteins. PTH caused a rapid, transient, decrease in myosin light chain phosphorylation and polymerization state of actin and myosin filaments, which seems to be mediated by cAMP.

MATERIALS AND METHODS

Bio-Lyte 4/6, urea, and molecular weight standards were from Bio-Rad, Richmond, CA; 1-34 and 3-34 parathyroid hormone peptides (human sequence) were from Bachem Corp., Torrance, CA; antibiotic A-23187 and Quin-2/AM were from Calbiochem-Behring Corp., La Jolla, CA; W-7 [N-(6-aminohexyl)-5-chloro-1-napthalenesulfonamide] was from Diversified Biotech, Boston, MA; Nunclon 4-well tissue culture dishes were from Nunc, Roskilde, Denmark; tissue culture dishes (100 × 20 mm) and (60 × 15 mm) were from Costar, Cambridge, MA; [^{3}H]-adenine and [^{32}P]-orthophosphoric acid (HCl-free in water) were from New England Nuclear Corp., Boston, MA; F-12 medium, horse serum, and kanamycin sulfate were from GIBCO, Grand Island, NY; fetal calf serum was from KC Biological, Lanexa, KA; pregnant Sprague-Dawley rats were from Charles River Farms, Wilmington, MA; Aclar (dacron sheets) were from Allied Chemical Co., Morristown, NJ; Rhodamine-conjugated phalloidin was from Molecular Probes, Inc., Junction City, OR; rabbit anti-human myosin (nonmuscle) IgG and fluorescein-conjugated goat anti-rabbit IgG were purchased from Biomedical Technologies, Inc., Stoughton, MA; DNAse I, Triton X-100, dimethylsulfoxide (grade I), Collagenase (Type I), Hyualuronidase (Type I), Trypsin (Type III), ampholines Pharmalyte (pH 3–10) and Pharmalyte (pH 5–8), cytochalasin B, purified rabbit muscle actin and myosin, N-propyl gallate, and all other reagents used in this study were obtained from Sigma Chemical Co., St. Louis, MO. The antibody to myosin light chain 20 KD was the generous gift of Dr. James R. Sellars (NHLBI, NIH).

Isolation and Cell Culture of Fetal Rat Calvaria Osteoblasts

Primary cultures of fetal rat calvaria osteoblastic cells were obtained as described [18]. For all experiments, cells were trypsinized after 1 week in culture and plated into secondary cultures at approximately 50,000 cells/cm^2 in NUNC 4-well dishes (2 cm^2 surface area). Experiments were conducted the following day, when the adherent cells from parallel dishes were counted with a Coulter counter following mild trypsinization under direct observation. The average plating efficiency was 80%. The coefficient of variation for cell counts between culture wells was 5%.

[^{32}P]-Orthophosphate Labeling of Cell Proteins

Cultures containing around 50,000 cells/cm^2 were washed with 0.5 ml calcium and magnesium-free Hanks balanced salt solution (CMFH) and were incubated with 0.2 ml of serum-free F-12 medium which contained 0.2 mCi/ml of [^{32}P]-orthophosphoric acid for 2 h at 37°C. The labeling medium was aspirated, and the cell monolayer was washed once with 0.5 ml of CMFH followed by immediate addition of medium containing the agents listed in the legends to the figures and tables. The assay was stopped by aspirating the experimental medium followed by addition of 0.1 ml 9 M urea, 130 mM 2-mercaptoethanol, 2% ampholines, and 5% Nonidet P-40 prior to two-dimensional-gel electrophoresis. The ^{32}P-labeling of proteins was estimated with a Zeineh soft laser scanning densitometer from radioautographs.

Single- and Two-dimensional Gel Electrophoresis of Triton-Soluble and Insoluble Proteins

Triton-insoluble pellets were prepared for electrophoresis, and the mass (μg/culture) of actin and myosin was determined as previously described [18]. Two-dimensional gel electrophoresis was carried out using 0.2 ml of Pharmalyte ampholine, pH range 3–10, 0.25 ml of Bio-byte ampholine, pH range 4–6, and 0.05 ml of Pharmalyte ampholine, pH range 5–8, for electrofocusing.

Measurement of [^{3}H]-cAMP Levels in Osteoblastic Cells

The intracellular content of [^{3}H]-cAMP was estimated in cells in which the ATP pool was labeled with 1 μCi/ml [^{3}H]-adenine for 2 h at 37°C [19,20]. The cells were washed, and 2 ml of pre-warmed serum-free medium containing 100 nM PTH (1–34) was added at 37°C. The reaction was stopped by addition of ice-cold perchloric acid (final concentration 10%). After 30 min extraction, ^{3}H-cAMP was separated by the

method of Salomon et al. [21], using [^{32}P]-cAMP for estimating recovery.

Fluorescence Microscopy

Cells were plated into secondary cultures at 10,000 cells/cm^2 on Aclar coverslips. After 3 days, the cells were washed with CMFH and treated with vehicle or 100 nM parathyroid hormone for 5 min. Other cells on coverslips were treated for 10 min with 1.2 μM cytochalasin B. All procedures were performed at room temperature, and each step was followed by rinsing the cells three times with PBS. Cells were fixed with 1.0% paraformaldehyde in 0.1 M sodium cacodylate, pH 7.4, for 30 min and then permeabilized with 0.01% Nonidet P-40 in PBS for 30 min. A 1:20 dilution of rhodamine-conjugated phalloidin in PBS was added to each coverslip and incubated in the dark for 30 min. For visualizing myosin, the protocol from Biomedical Technologies, Inc., was used. Briefly, cells were fixed as above and dehydrated and permeabilized for 3 min in absolute acetone cooled to −20°C. A 1:25 dilution of the rabbit anti-myosin IgG was incubated with cells for 90 min. A 1:100 dilution of fluorescein-conjugated goat anti-rabbit IgG was added to the cells for 60 min in the dark. Before covering each Aclar coverslip with a glass coverslip, a drop of 2.5% n-propyl gallate [22] in a 1:1 PBS and glycerol solution was added. The samples were observed with a Leitz Dialux 20 microscope.

RESULTS

Effect of Parathyroid Hormone on Cytoskeletal Actin and Myosin

The major proteins obtained in the Triton X-100 insoluble pellet were primarily those of the cytoskeleton, in particular, actin and myosin (Fig. 1) [18,23]. Treatment of cells with PTH caused a dose-dependent decrease in the actin and myosin associated with the Triton insoluble

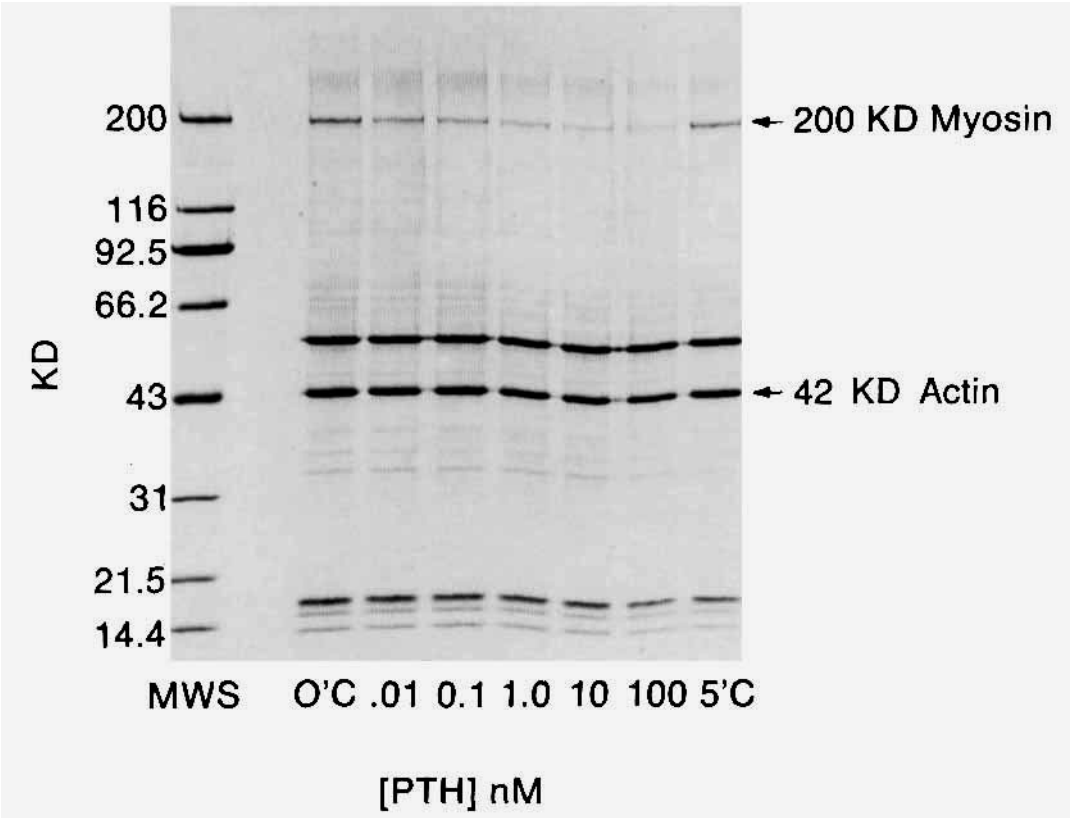

Fig. 1. SDS gradient gel electrophoresis of Triton-insoluble proteins isolated after treatment of osteoblasts with increasing concentrations of parathyroid hormone. Cells were plated into Nunc dishes at 50,000 cells/cm^2. Twenty-four hours later, the cells were treated for 5 min with increasing concentrations of parathyroid hormone (PTH) and the Triton-insoluble proteins were processed as described in Materials and Methods. MWS, molecular weight standards; **lane O'C,** 0 min control; **following lanes:** 5 min treatment with PTH at the indicated concentrations; **lane 5'C,** 5 min treatment with vehicle (0.001% NaAc plus 0.001% BSA in F-12 medium). This is a representative gel of six replicate experiments.

pellet of the cytoskeleton. Figure 1 shows a representative gel from six experiments. The mean values from two experiments are presented in Figure 2. The IC_{50} for the PTH effect on both actin (panel A) and myosin (panel B) was approximately 1 nM, and the saturation dose was approximately 100 nM. The PTH dose-response curve was shifted to the right and the IC_{50} increased by an order of magnitude in the presence of 100 nM PTH antagonist [3–34(8,18)-norleu 34 tyrosine], a competitive inhibitor of PTH [24] (Fig. 2, panels C and D).

The PTH-induced decrease in the amount of actin and myosin associated with the Triton-insoluble cytoskeleton was transient and reached its nadir at 5–10 min (Fig. 3). Actin decreased from 19 ± 0.4 pg/cell to 13 ± 0.5 pg/cell, and myosin decreased from 5 ± 0.4 pg/cell to 2 ± 0.5 pg/ml. The change in myosin was detected at 30 s and preceded that of actin. The mass of both proteins in the cytoskeletal fraction started returning toward control levels at 10 min. Cytoskeletal actin reached control levels at 20–30 min, while cytoskeletal myosin remained below initial levels for at least 6 h. The molar ratio of actin and myosin associated with the cytoskeletal pellet was about 18 at 0 min, 24 at 2 min, 32 at 10 min, and 26 at 20 min.

Figure 4 shows the time course for cAMP changes following the addition of 100 nM PTH in the absence of phosphodiesterase inhibitors. The cAMP level increased almost linearly for 4 min and declined rapidly thereafter. A similar time course was observed for cellular cytoskeletal actin and myosin content, which reached a nadir at around 5 min.

Cytochemical Visualization of F-actin and Myosin

Phalloidin staining of control cells demonstrated numerous microfilament bundles or stress fibers traversing the cytoplasm and running parallel to each other (Fig. 5A). Some cells had concentrically arranged, thick fibers from which thinner, radially arranged microfilament

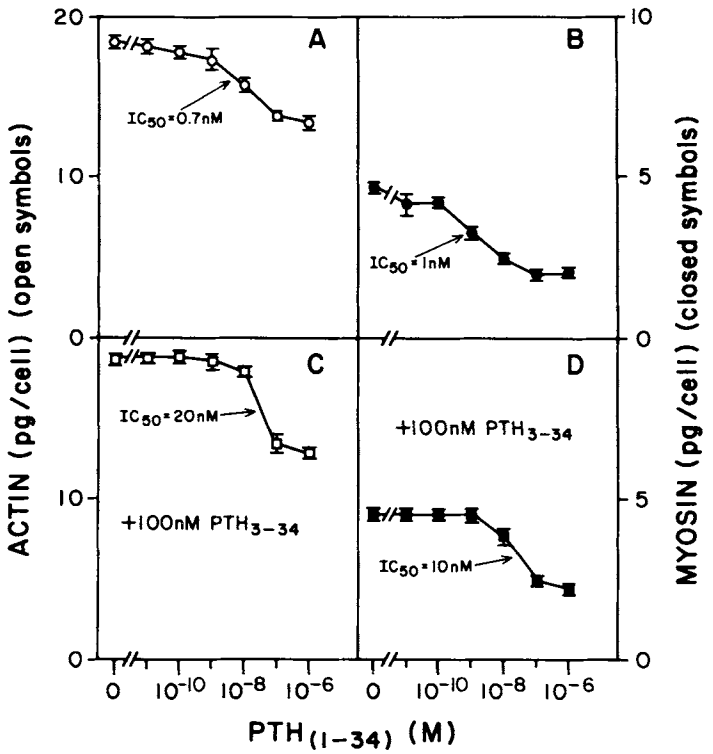

Fig. 2. Dose-response curve for the effect of parathyroid hormone on Triton-insoluble actin and myosin; antagonism of (3–34) PTH. Cells were plated into Nunc dishes at 50,000 cells/cm^2. Twenty-four hours later, the cells were washed and treated for 5 min at 37°C with the indicated concentrations of PTH agonist in the absence (**panels A, B**) or presence (**panels C, D**) of 100 nM PTH antagonist. The cells were processed, and the mass of Triton-insoluble actin (open symbols, panels A, C) and myosin (closed symbols, panels B, D) were quantitated as described in Materials and Methods. The 0 (zero) data point represents the 5 min control sample. Data are expressed as pg/cell Triton-insoluble actin and myosin and represent mean ± SEM of duplicate samples from two experiments.

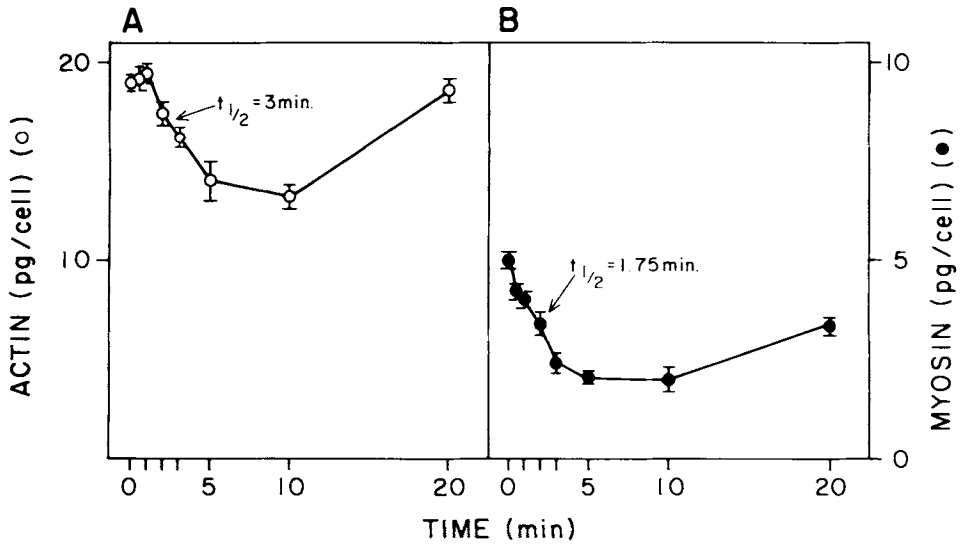

Fig. 3. Time course for the effect of parathyroid hormone on the mass of Triton-insoluble actin and myosin. Cells were plated into Nunc dishes at 50,000 cells/cm^2. Twenty-four hours later, the cells were washed and treated with 100 nM parathyroid hormone. The Triton-insoluble proteins were separated at the indicated times and processed as described in Materials and Methods. Data are expressed as pg/cell Triton-insoluble actin and myosin. The time-dependent decrease in the mass of Triton-insoluble actin is shown in **Panel A** (open symbols); that for myosin in **Panel B** (closed symbols). Data represent mean ± SEM of triplicate samples from triplicate experiments.

bundles projected into the ruffled edge of the cell. Most cells appeared well spread.

Stimulation with 10^{-8} M PTH for 1 or 5 min produced a dramatic rearrangement of the cytoskeleton and a change in the shape of 40–50% of the cells (Fig. 5B). A decrease in the total number of stress fibers per cell was seen. With 10^{-8} to 10^{-10} M PTH, the percentage of cells demonstrating this rearrangement of microfilaments decreased in a dose-dependent manner (data not shown). Stained aggregates were found throughout the cell with a preponderance of the aggregates in the perinuclear region and/or at the leading edge of the cells. Similar aggregates were seen in cells treated with cytochalasin B (Fig. 5C). The PTH-treated cells also became stellate-shaped, were less spread than the control cells, and had long thin processes, which appeared to be retracting. These retracting processes were not seen very often in the cytochalasin B-treated cells that appeared to collapse and became irregularly shaped (Fig. 5C).

Fluorescent labeling of myosin demonstrated a punctate labeling of parallel microfilaments throughout the cytoplasm with some aggregation in the perinuclear region (Fig. 6A). Administration of 10^{-8} M PTH for 5 min increased the staining in the perinuclear region and decreased the number of microfilaments (Fig. 6B).

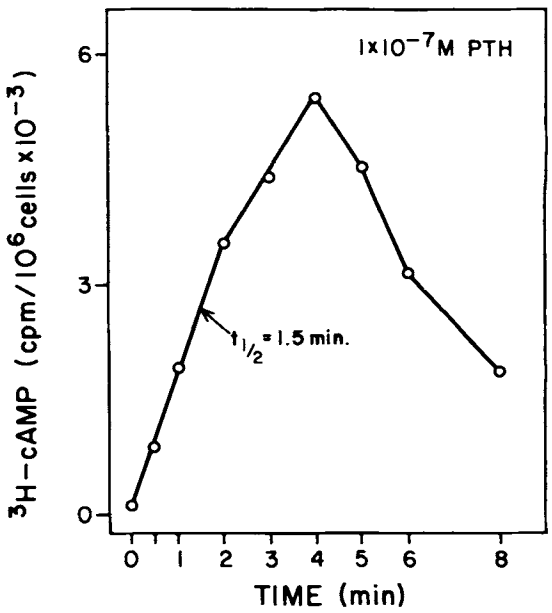

Fig. 4. Time course for accumulation of cAMP in osteoblastic cells. Cells were plated into 60 mm culture dishes at 1.5 × 10^6 cells/dish (60,000 cells/cm^2). Twenty-two hours later, the cells were labeled with 1 μCi/ml [^{3}H]-adenine for 2 h at 37°C. At the end of the labeling period, the cells were washed and 2 ml serum-free medium containing 100 nM parathyroid hormone was added at 37°C. The reaction was stopped at the indicated times and [^{3}H]-cyclic AMP was determined as described in Materials and Methods. Data represent mean of triplicate samples. Data are expressed as cpm [^{3}H]-cAMP/10^6 cells × 10^{-3}. Arrow points to the half-time for the rise in cyclic AMP.

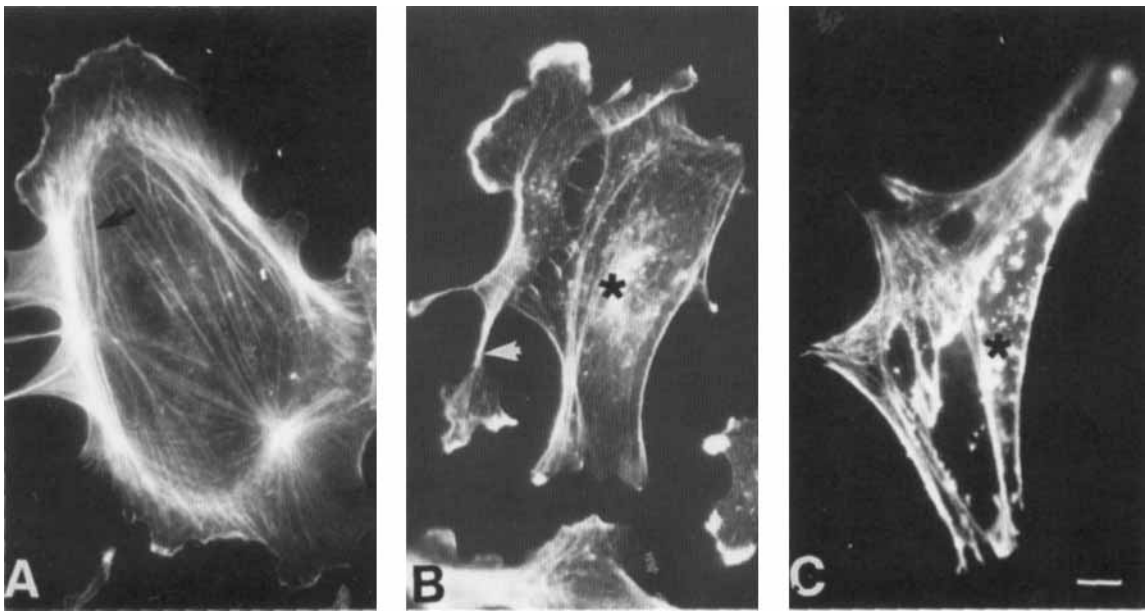

Fig. 5. The effect of parathyroid hormone and cytochalasin B on the phalloidin staining pattern of microfilaments. Secondary cultures were treated with vehicle (**A**) for 5 min, 100 nM parathyroid hormone (**B**) for 5 min, or 1.2 μM cytochalasin B (**C**) for 10 min. Phalloidin staining of the microfilaments demonstrated numerous microfilament bundles (arrow) in the control cells. A decrease in the number and diameter of microfilaments and the aggregation of phalloidin-staining material in the perinuclear region (asterisk) were apparent in parathyroid hormone-treated cells (B). Hormone-treated cells were less spread than the control cells and had thin retracting processes (arrowhead). Cytochalasin B treatment (C) also produced phalloidin-stained aggregates (asterisk) and a change in cell shape. Bar = 10 μm.

The Effect of Quin-2/AM

The possible role of intracellular calcium on the disruption of the cytoskeleton was tested by equilibrating the cells with the calcium chelating buffer Quin-2/AM [25] at 1.0 and 10 μM (or vehicle). As seen in Table I, 10 μM Quin-2 caused a 40% decrease in cytoskeletal actin and a 50% decrease in cytoskeletal myosin. The calmodulin antagonist W-7 similarly caused a reduction in cytoskeletal proteins, while phorbol myristate acetate, which stimulates protein kinase C, had no effect (data not shown).

Effect of PTH on Myosin Light Chain Phosphorylation

A phosphorylated protein with a molecular weight of 20 kD and a pI of 4.85–5.00 was identified by two-dimensional gel electrophoresis and Western blots as the myosin light chain (Fig. 7). This protein was present in the Triton-insoluble cytoskeletal fraction of [^{32}P]-labeled cells. The effect of PTH on the phosphorylation state of that protein as a function of time is shown in the autoradiograms of Figure 8a (arrow, panels A–I). The results obtained by scanning densitometry of autoradiograms from five such experiments, presented in Figure 8b, show that PTH caused a rapid transient reduction in the phosphorylation of MLC, reaching about 50% of control at 2 min and returning to 80% of control levels at 5 min. Since the PTH effects on cytoskeletal actin and myosin were mimicked by the calcium chelating buffer Quin-2, we examined if a reduction in intracellular calcium was necessary for the PTH-induced decrease in myosin light chain phosphorylation.

Cells in F-12 medium (1.1 mM calcium) were treated with PTH in the absence or presence of the calcium ionophore A-23187. As shown in Figure 9, 100 nM PTH (1–34) reduced the phosphorylation of the 20 kD, pI 4.85–5.0, protein (panels D, E, F, relative to A, B, C) both in the absence (panels A, D) and in the presence of 0.3 μM (panels B, E) or 1.0 μM (panels C, F) A-23187 ionophore. The phosphorylation of two unidentified proteins (1 and 2) in the boxed region, left panel, of 33.6 kD (pI 4.9 and 5.05, respectively) increased in the presence of A-23187. Phosphorylation was estimated by soft-laser densitometry of autoradiograms relative to a protein, la-

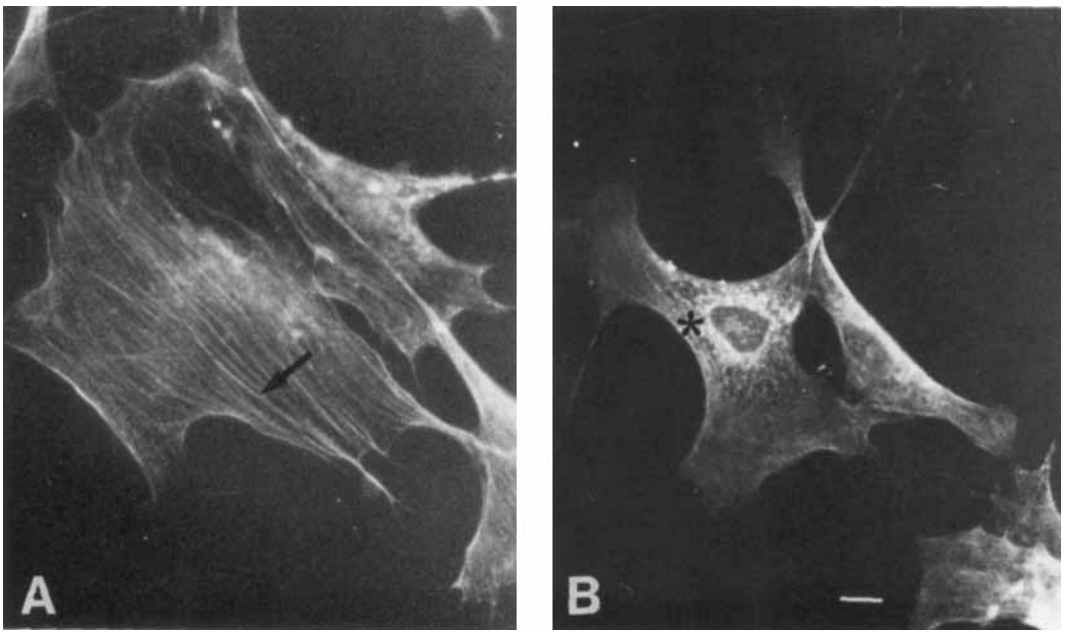

Fig. 6. The effect of parathyroid hormone on the myosin staining pattern. Secondary osteoblast cultures were treated with vehicle (**A**) or 100 nM parathyroid hormone (**B**) for 5 min. Staining of the myosin by immunofluorescence revealed numerous filaments in parallel arrays (arrow) in the control cells (A). With hormone treatment (B), few filaments were found and a patchy fluorescence pattern was seen in the perinuclear region (asterisk). Bar = 10 μm.

beled "a," which did not change during these treatments. The graphic representation of the means is presented above the autoradiograms for proteins 1 and 2 and below for "a" and MLC.

DISCUSSION

This study confirms previous reports on PTH-induced changes in the shape and in the microfilament pattern of osteoblastic cells [5–7]. We found that these changes were associated with a rapid reduction in the cytoskeletal actin and myosin, operationally defined as that which was not extractable with 1% Triton X-100. At saturating PTH concentrations, about 50% of the cytoskeletal actin and myosin became Triton X-100 extractable. A similar fraction became extractable after addition of cytochalasin B, which promotes microfilament disassembly by preventing actin assembly [26–28]. This fraction did not increase when both agents were administered together, suggesting that there is a limited, common pool of microfilaments that are subject to the action of these agents.

TABLE 1. The Effect of Quin-2/AM Loading on Cytoskeletal Actin and Myosin in Osteoblastic Cells

Condition	Actin (pg/cell)	Myosin (pg/cell)
0 min control	18.7 ± 1.60	4.80 ± 0.40
Quin-2/AM		
(1.0 μM)	16.83 ± 1.24	3.84 ± 0.65
(10.0 μM)	11.22 ± 0.70	2.40 ± 0.30
30 min control	19.1 ± 1.30	5.05 ± 0.65

Cells were plated into Nunc dishes at 45,000 cells/cm^2. Twenty-four hours later, the cells were washed, followed by loading with Quin-2/AM in DMSO vehicle or vehicle alone. After 30 min, Triton X-100 medium was added and the cytoskeleton proteins were separated, processed through SDS/PAGE, and the mass of actin and myosin quantitated as described in Materials and Methods. Data is expressed as pg/cell actin or myosin (±) SEM of quadruplicate determinations.

Several findings suggest that the transition from cytoskeletal to extractable actin and myosin was myosin-regulated [17,29]. Assuming equal sensitivity for the detection of the two proteins, myosin depolymerization seems to precede that of actin: The ratio of non-extractable (polymerized) actin to myosin, which was 18 in the resting state, increased to 24 and 32 during depolymerization. A phosphorylated protein identified as myosin light chain (MLC) was rapidly dephosphorylated following PTH addition. The rapid dephosphorylation paralleled the rapid decrease in actin and myosin associated with the

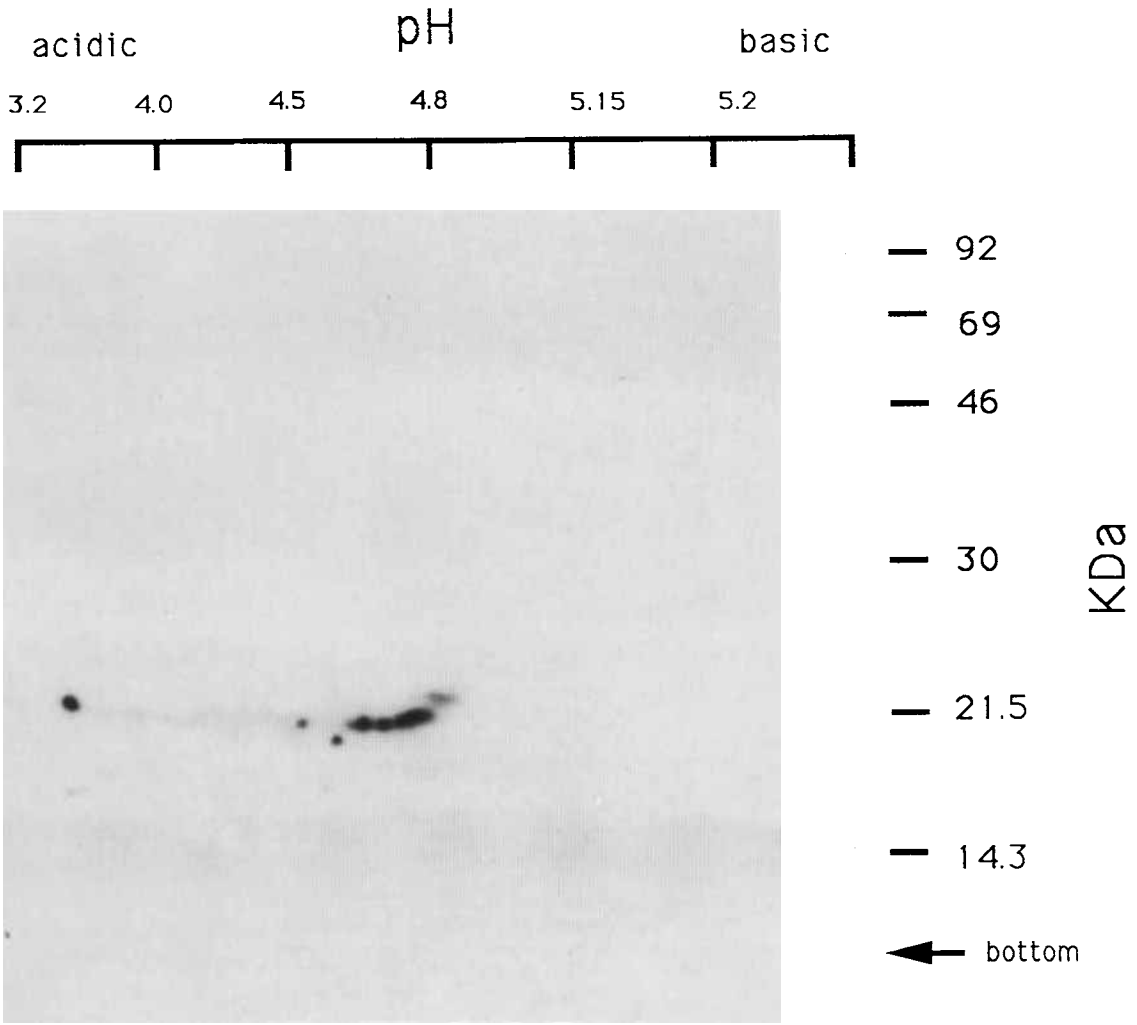

Fig. 7. Identification of myosin light chain in osteoblastic cells by Western immunoblot analysis. Cells were cultured, and cytoskeletal proteins were extracted as described in Materials and Methods. Protein samples were first processed by isolectric focusing, as described in Materials and Methods, followed by 12.5% acrylamide SDS-PAGE (second dimension). The gels were electroblotted onto nitrocellulose overnight at 50 V, 4°C. The blots were incubated with antibody to myosin light chain (1:50 dilution), followed by incubation with ^{125}I-protein A and autoradiography.

Triton-insoluble cytoskeleton. However, the repolymerization of myosin and actin considerably lagged behind the rephosphorylation of MLC, 20–30 min vs. 5 min, suggesting that the reassociation of actin and myosin with the cytoskeleton may involve another process or other cytoskeletal components that require more time for completion. Alternatively, after PTH stimulation, the cytoskeleton is rearranged in a form that is different from that in untreated cells.

The changes in MLC phosphorylation can be detected 0.5 min after hormone addition, making it the earliest reported effect of PTH following the stimulation of adenylate cyclase and protein kinase A.

PTH was also reported to raise intracellular calcium levels in its target cells [30,31], and both calcium and cyclic AMP have been implicated in the regulation of cytoskeletal disassembly, by having opposite effects on myosin light chain kinase (MLCK). In smooth muscle and platelets, MLCK activity is increased by calcium/calmodulin and reduced by A-kinase mediated phosphorylation. A rise in cyclic AMP would thus lead to disassembly of the cytoskeleton, whereas a fall in cyclic AMP, resulting in A-kinase inactivation

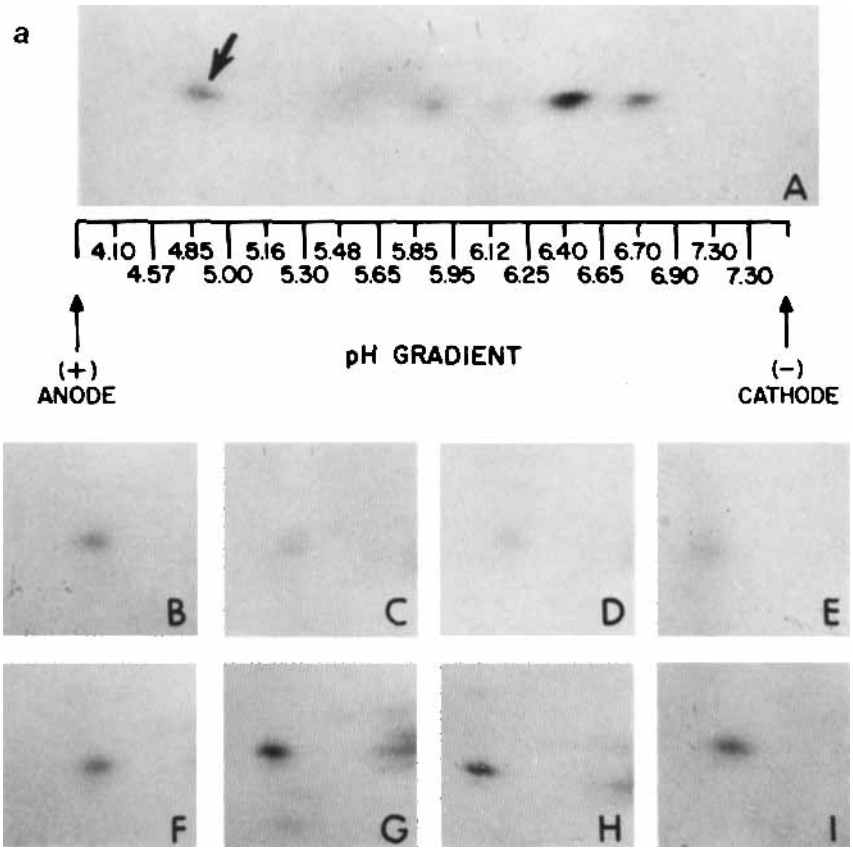

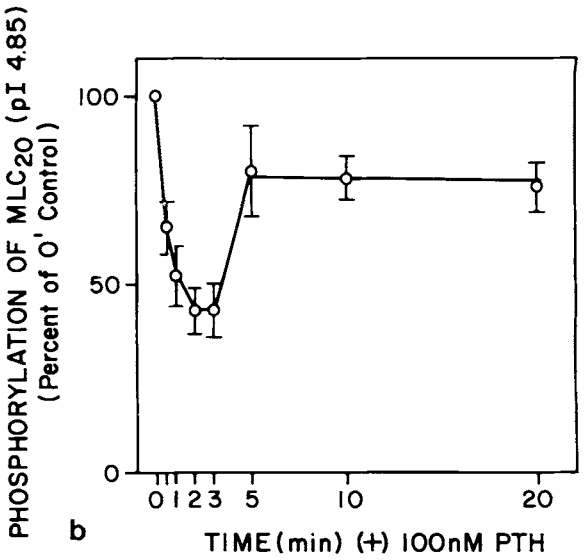

Fig. 8. Time course for the effect of parathyroid hormone on MLC phosphorylation. Cells were plated into Nunc dishes at 52,000 cells/cm^2. Twenty-two hours later, the cells were labeled with [^{32}P]-orthophosphate, and 2 h later, were washed and treated with 100 nM parathyroid hormone (PTH) for the times indicated, then the whole cells were lysed and processed through 2-D gel electrophoresis and autoradiography as described in Materials and Methods. All dried gels were subjected to autoradiography at the same time. **a: Top panel** represents autoradiograph from the lower portion of the second dimension of 2-D gel (slab gel molecular weight range approximately 20 KD). Arrow in **panel A** points to 20 KD, pI 4.85–5.00 protein (MLC), shown below in panels **B** to **I.** A: 0 min control; panels B–I, plus 100 nM PTH; B: 0.5 min; C: 1.0 min; D: 2.0 min; E: 3.0 min; F: 4.0 min; G: 5.0 min; H, 10 min; I: 20 min. This is representative of five independent experiments. **b:** Five independent experiments were carried out as described in a. The data represent mean ± SEM for values of the 20 KD, pH 4.9, MLC spot from these experiments, estimated by densitometry, expressed as % of 0 minute control.

[32], would lead to reassembly. A close correlation between the onset of physiological response (lipolysis) and the activation state of cAMP-dependent protein kinase was also demonstrated in adipocytes [33].

In the present study, cyclic AMP is the likely mediator of PTH effects on the cytoskeleton since agents that increase intracellular cyclic AMP had similar effects to those of PTH [18]. There was no direct correlation between the magnitude of cAMP and cytoskeletal changes, which were already maximal following a twofold elevation in cAMP, produced by IBMX. This is not surprising since very small changes in cAMP

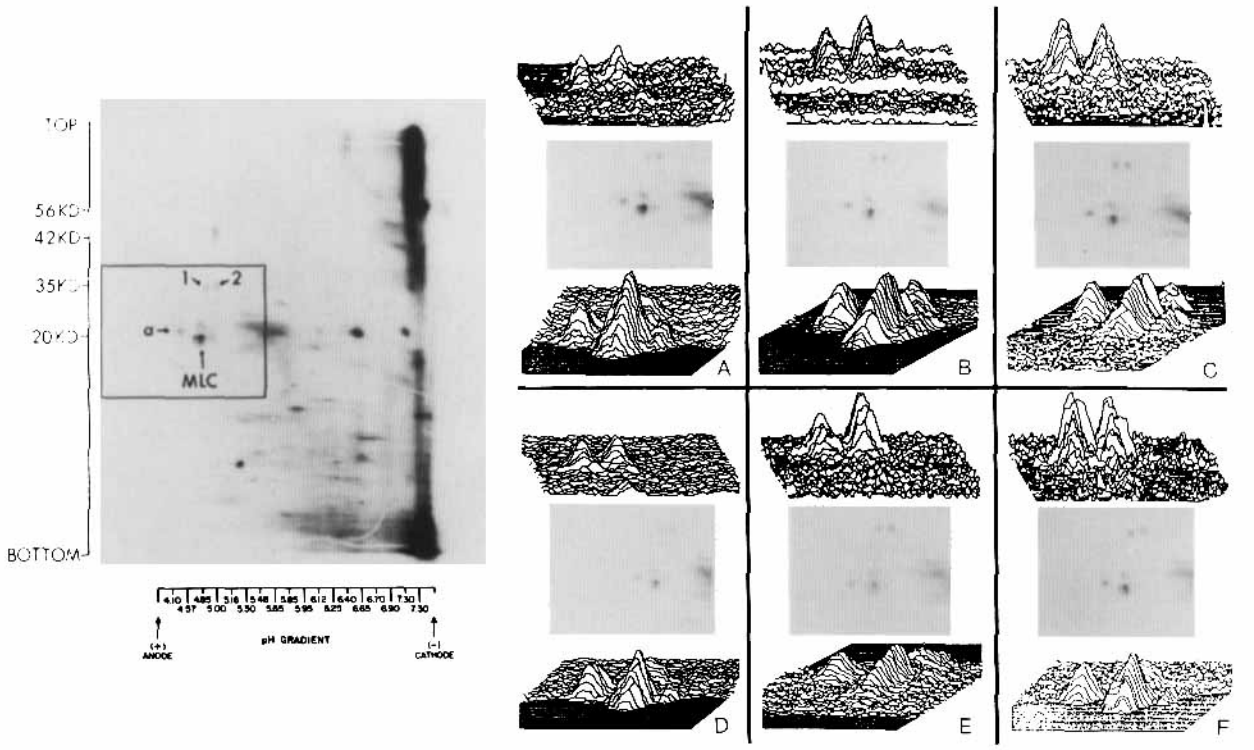

Fig. 9. Autoradiography of [^{32}P]-labeled proteins. Effect of parathyroid hormone on the phosphorylation state of MLC and other proteins in the absence and presence of ionophore A-23187. Cells were plated into Nunc dishes at 47,000 cells/cm^2. Twenty-two hours later, cells were labeled with [^{32}P]-orthophosphate as described in Materials and Methods. Two hours later, cells were washed and treated with 100 nM parathyroid hormone (PTH) for 2 min and/or A23187, as described below. Whole cells were lysed, processed through 2-D gel electrophoresis (second dimension, 15% SDS slab gel), followed by autoradiography and soft laser densitometry, to obtain 3-D graphics from which integrated volumes of peaks were obtained. The **left panel** represents an autoradiograph of the whole 2-D gel. The scale on the left margin refers to molecular weights; that on the bottom, to the pH gradient, from anode to cathode. The section included within the square is the area of autoradiographs, presented in **panels A–F.** The following proteins indicated by arrows were scanned: Spot 1, 33.6 KD, pI 4.90; Spot 2, 33.6 KD, pI 5.10; Spot a, 21 KD, pI 4.40; MLC, 20 KD, pI 4.85–5.00. Treatment of cells was as follows: **Left large panel:** 0 min control; A: 2 min control; B: 0.3 μM A23187; C: 1 μM A23187; D: 100 nM PTH; E: 100 n MPTH + 0.3 μM A23187; F: 100 nM PTH + 1 μM A23187. The graphics at the top of the autoradiograph in each panel present the integrated intensity of Spots 1 and 2, respectively, while those at the bottom of each panel present the integrated intensity for Spot "a" and MLC, respectively.

were shown to cause maximum stimulation of protein kinase A in these cells [34]. The time course for PTH-induced cAMP changes is consistent with cyclic AMP mediation, and intracellular calcium was reported to increase, rather than to decrease, in response to PTH [29,30].

However, the reduction of intracellular calcium by Quin-2A, as well as the calmodulin antagonist W-7 [35], which may interact directly with MLC [36], also caused disassembly. To further examine the relationship between cAMP and calcium in the action of PTH on the cytoskeleton, we followed the state of phosphorylation of MLC after PTH addition, in the presence and absence of the calcium ionophore A-23187. We found that even in the presence of A-23187, which increased the phosphorylation of a couple of unknown proteins, presumably via a calcium-dependent protein kinase, PTH addition still reduced the phosphorylation of MLC. These findings support the role of cAMP in the mediation of PTH action in this system and suggest a sequence of events similar to that described in smooth muscle [16].

An alternate, mutually non-exclusive, explanation for MLC dephosphorylation following PTH addition could be the activation of MLC phosphatases by cyclic AMP. Phosphatases, which act on MLC, have been isolated from smooth muscle [37] and phosphatase activation by cyclic

AMP has been reported in S49 cells [38]; however, it has not been shown that the MLC phosphatases are subject to cAMP activation.

MLC phosphorylation actually starts rising prior to the return of cAMP to baseline levels. Phosphorylation of MLC by another kinase, such as protein kinase C, has been reported and could explain these findings [39]. Multiple-site phosphorylation on smooth muscle myosin has also been reported [40]. The reassembly of proteins following MLC rephosphorylation is considerably delayed and could be due to calcium-dependent activation of gelsolin [41]. These are just several possible explanations for these observations, consistent with the available information.

The role of the PTH-induced changes in the cytoskeleton and shape of osteoblasts is not known. It was proposed that changes in the shape of bone lining cells may participate in PTH stimulation of bone resorption [42]. In several cell types, including mesenchymal cells of similar developmental origin as osteoblasts, such as chondroblasts and adipocytes, shape changes were shown to regulate the expression of genes related to differentiation [43–45]. These shape and cytoskeletal changes may be part of a "pleiotropic" response to PTH or could play a specific role(s), which remains to be determined, in the mechanism of action of this hormone.

ACKNOWLEDGMENTS

We thank Mr. William Grasser for his help with the photography and Ms. Dianne McDonald for preparation of the manuscript.

REFERENCES

1. Rappaport B, Jones AL: Endocrinology 102:175–181, 1978.
2. Westermark B, Porter KR: J Cell Biol 94:42–50, 1983.
3. Spruill WA, White MG, Steiner AL, Tres LL, Kierszenbaum AL: Exp Cell Res 131:131–148, 1981.
4. Cheitlin R, Ramachandran J: J Biol Chem 256:3156–3158, 1981.
5. Jones SJ, Boyde A: Cell Tissue Res 169:449–465, 1976.
6. Miller SS, Wolf AM, Arnaud CD: Science 192:1340–1343, 1976.
7. Aubin JE, Alders E, Heersche JNM: Exp Cell Res 143: 439–450, 1983.
8. Puck TT, Waldren CA, Hsie AW: Proc Natl Acad Sci USA 69:1943–1947, 1972.
9. Porter KR, Puck TT, Hsie AW, Kelley D: Cell 2:145–162, 1974.
10. Bloom GS, Lockwood AH: Exp Cell Res 129:31–45, 1980.
11. Korn ED: Proc Natl Acad Sci USA 75:588–599, 1978.
12. Adelstein RS: Cell 30:349–350, 1982.
13. Adelstein RS, Conti MA: Nature 256:597–598, 1975.
14. Sellers JR, Pato MD, Adelstein RS: J Biol Chem 256: 13137–13142, 1981.
15. Hathaway DR, Adelstein RS: Proc Natl Acad Sci USA 76:1653–1657, 1979.
16. Adelstein RS, Conti MA, Hathaway DA, Klee CB: J Biol Chem 253:8347–8350, 1978.
17. Feinstein MB, Egan JJ, Opas EE: J Biol Chem 258:1260–1267, 1983.
18. Egan JJ, Gronowicz G, Rodan GA: Submitted.
19. Humes JL, Rounbehler M, Kuehl F Jr: Anal Biochem 32:210–217, 1969.
20. Rodan SB, Insogna KL, Vignery AMC, Stewart AF, Broadus AE, D'Souza SM, Bertolini DR, Mundy GR, Rodan GA: J Clin Invest 72:1511–1515, 1983.
21. Salomon Y, Londos C, Rodbell M: Anal Biochem 58:541–549, 1974.
22. Giloh H, Sedat JW: Science 217:1252–1255, 1982.
23. Rosenberg S, Stratcher A, Lucus RC: J Cell Biol 91:201–211, 1981.
24. Rosenblatt M, Callahan EN, Mahaffey JE, Pont A, Potts JT Jr: J Biol Chem 252:5847–5851, 1977.
25. Tsien RY: Biochemistry 19:2396–2404, 1980.
26. Fox JEB, Phillips DR: Nature 292:605–652, 1981.
27. White JR, Naccache PH, Sha'afi RI: J Biol Chem 258: 14041–14047, 1983.
28. MacLean-Fletcher S, Pollard TD: Cell 20:329–341, 1980.
29. Fox JEB, Phillips DR: J Biol Chem 257:4120–4126, 1982.
30. Yamaguchi DT, Hahn TJ, Iida-Klein A, Kleeman CR, Muallem S: J Biol Chem 262:7711–7718, 1987.
31. Lieberherr M: J Biol Chem 27:13168–13173, 1987.
32. Corbin JD, Keely SE, Soderling TR, Park CR: Adv Cyclic Nucleotide Res 5:265–279, 1979.
33. Londos C, Honnor RC, Dhillon GS: J Biol Chem 260: 15139–15145, 1985.
34. Partridge NC, Kemp BE, Veroni MD, Martin TJ: Endocrinology 108:220–225, 1981.
35. Hidaka H, Asano M, Ivadore S, Matsumoto I, Tosuka T, Aoki N: J Pharmacol Exp Ther 207:8–15, 1978.
36. Zimmer M, Hofmann F: Eur J Biochem 142:393–397, 1984.
37. Pato MD, Kerc E: J Biol Chem 260:12359–12366, 1985.
38. Kiss Z, Steinberg RA: FEBS Lett 180:207–211, 1985.
39. Naka M, Nishikawa M, Adelstein RS, Hidaka H: Nature 306:490–492, 1983.
40. Ikebe M, Hartshorne DJ, Elzinga M: J Biol Chem 261: 36–39, 1986.
41. Yin HL, Zaner KS, Stossel TP: J Biol Chem 255:9494–9500, 1980.
42. Rodan GA, Martin TJ: Calcif Tissue Int 33:349–351, 1981.
43. Aggeler J, Frisch SM, Werb Z: J Cell Biol 98:1662–1671, 1984.
44. Spiegelman BM, Ginty CA: Cell 35:657–666, 1983.
45. Benya PD, Brown PD, Padilla SR: J Cell Biol 106:161–170, 1988.